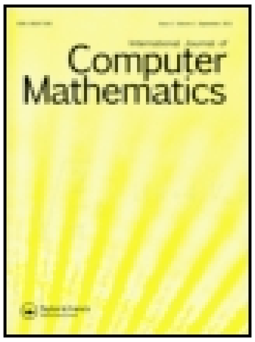

International Journal of Computer Mathematics

ISSN: 0020-7160 (Print) 1029-0265 (Online) Journal homepage: http://www.tandfonline.com/loi/gcom20

Variational phase recovering without phase unwrapping in phase-shifting interferometry

Ricardo Legarda-Saenz, Alejandro Téllez Quiñones, Carlos Brito-Loeza & Arturo Espinosa-Romero

INTERNATIONAL JOURNAL OF COMPUTER MATHEMATICS
https://doi.org/10.1080/00207160.2018.1499899

Taylor & Francis
Taylor & Francis Group

Variational phase recovering without phase unwrapping in phase-shifting interferometry

Ricardo Legarda-Saenz [a], Alejandro Téllez Quiñones [b], Carlos Brito-Loeza [a] and Arturo Espinosa-Romero [a]

[a]CLIR at Facultad de Matemáticas, Universidad Autónoma de Yucatán, Mérida, México; [b]CONACYT-Centro de Investigación en Ciencias de Información Geoespacial, A.C. Unidad Mérida, Sierra Papacal, México

ABSTRACT
We present a variational method for recovering the phase term from the information obtained from phase-shifting methods. First we introduce the new method based on a variational approach and then describe the numerical solution of the proposed cost function, which results in a simple algorithm. Numerical experiments with both synthetic and real fringe patterns show the accuracy and simplicity of the resulting algorithm.

ARTICLE HISTORY
Received 22 March 2018
Revised 4 June 2018
Accepted 23 June 2018

KEYWORDS
Fringe analysis; image reconstruction techniques; phase retrieval

2010 MSC SUBJECT CLASSIFICATIONS
78A99; 68U10; 65K10; 65N22; 65F22

1. Introduction

The main goal of fringe analysis techniques is to recover accurately the modulated phase from one or several fringe patterns [19,20]; such phase is related to some physical quantities such as shape, deformation, refractive index and temperature. The basic model for a fringe pattern is given by

$$I_{\mathbf{x}} = a_{\mathbf{x}} + b_{\mathbf{x}} \cos\left(\phi_{\mathbf{x}}\right),$$

where $\mathbf{x} = (x, y)$, $a_{\mathbf{x}}$ is the background illumination, $b_{\mathbf{x}}$ is the amplitude modulation and $\phi_{\mathbf{x}}$ is the phase map to be recovered.

Among the methods for phase estimation is the phase-shifting method [3,23], which consists in acquiring several fringe patterns where the phase term is incremented between successive frames. Such fringe patterns are defined as

$$I_{\mathbf{x},k} = a_{\mathbf{x}} + b_{\mathbf{x}} \cos\left(\phi_{\mathbf{x}} + \alpha_k\right), \quad k = 1, \ldots, K, \quad K \geq 3,$$

where α_k is the phase step and K is the number of fringe patterns used. For every α_k, the fringe pattern can be written as

$$I_{\mathbf{x},k} = a_{\mathbf{x}} + b_{\mathbf{x}} \cos\left(\phi_{\mathbf{x}} + \alpha_k\right) = I^0_{\mathbf{x}} + I^c_{\mathbf{x}} \cos\left(\alpha_k\right) - I^s_{\mathbf{x}} \sin\left(\alpha_k\right), \tag{1}$$

where

$$I^0_{\mathbf{x}} = a_{\mathbf{x}},$$

CONTACT Ricardo Legarda-Saenz rlegarda@correo.uady.mx CLIR at Facultad de Matemáticas, Universidad Autónoma de Yucatán, Anillo Periférico Norte, Tablaje Cat. 13615, C.P. 97203 Mérida, Yucatán, México

$$I^c_{\mathbf{x}} = b_{\mathbf{x}} \cos(\phi_{\mathbf{x}}),$$
$$I^s_{\mathbf{x}} = b_{\mathbf{x}} \sin(\phi_{\mathbf{x}}).$$

The functions $I^0_{\mathbf{x}}, I^c_{\mathbf{x}}, I^s_{\mathbf{x}}$ can be estimated with different phase-shifting techniques [26,27,31–33]. Using these coefficients, the wrapped phase term can be computed by [14]

$$\hat{\phi}_{\mathbf{x}} = \mathtt{atan2}\left[I^s_{\mathbf{x}}, I^c_{\mathbf{x}}\right] = \phi_{\mathbf{x}} \bmod 2\pi. \tag{2}$$

Then the phase term $\phi_{\mathbf{x}}$ is estimated by a process named phase unwrapping [5], which is usually computationally intensive and susceptible to noise. To avoid these drawbacks, several approaches have been developed to estimate the phase without the need of the unwrapping process [11,12,22,30].

A different approach is found in reference [17], where the information obtained from the phase-shifting method, given in Equation (1), is used to estimate the phase term $\phi_{\mathbf{x}}$ from the information of $I^c_{\mathbf{x}}$ and $I^s_{\mathbf{x}}$, and the partial derivatives of these two functions, respectively. This approach consists in computing the gradient field as follows:

$$\Phi_{\mathbf{x}} = \left(\Phi^1_{\mathbf{x}}, \Phi^2_{\mathbf{x}}\right) = \left(\frac{\partial \phi_{\mathbf{x}}}{\partial x}, \frac{\partial \phi_{\mathbf{x}}}{\partial y}\right) = \left(\frac{\frac{\partial I^s_{\mathbf{x}}}{\partial x} I^c_{\mathbf{x}} - I^s_{\mathbf{x}} \frac{\partial I^c_{\mathbf{x}}}{\partial x}}{\left(I^c_{\mathbf{x}}\right)^2 + \left(I^s_{\mathbf{x}}\right)^2}, \frac{\frac{\partial I^s_{\mathbf{x}}}{\partial y} I^c_{\mathbf{x}} - I^s_{\mathbf{x}} \frac{\partial I^c_{\mathbf{x}}}{\partial y}}{\left(I^c_{\mathbf{x}}\right)^2 + \left(I^s_{\mathbf{x}}\right)^2}\right). \tag{3}$$

From the gradient field $\Phi_{\mathbf{x}}$, the phase term $\phi_{\mathbf{x}}$ is estimated by using line integrals [17]. In this way, the nonlinearity of the arctangent function, Equation (2), is avoided. This approach has been successfully used on the demodulation of fringe patterns obtained from phase-shifting methods [27,28]. However, the line integrals approach fails with moderate levels of noise and/or aliasing in the input fringe patterns, in the same way the Itoh's method does [5].

In this work, we present a method for recovering the phase term $\phi_{\mathbf{x}}$ from the information obtained from phase-shifting methods; that is, using only the fringe patterns $I^c_{\mathbf{x}}$ and $I^s_{\mathbf{x}}$, avoiding the use of the nonlinear arctangent function. First we introduce the new method based on a variational approach. Then we describe the numerical solution of the proposed cost function, which results in a simple algorithm. The performance of the proposed method is evaluated by numerical experiments with both synthetic and real data. A comparison against two well-known least-square based unwrapping methods is also presented. Finally we discuss our results and present some concluding remarks.

2. A new variational model for the recovery of the phase from phase-shifting method

2.1. Variational formulation

Variational techniques have been successfully used in fringe pattern processing. In the literature, it is possible to find several works about fringe-pattern filtering [13,34,35], demodulation [12], unwrapping [10] and gradient-field estimation of a wrapped-phase for unwrapping processing [7].

In this work, we propose to estimate the phase map $\phi_{\mathbf{x}}$ as the solution of the minimization problem defined by

$$\min_{\phi} E(\phi_{\mathbf{x}}), \tag{4}$$

where

$$E(\phi_{\mathbf{x}}) = \frac{1}{2}\int_{\Omega} |\nabla \phi_{\mathbf{x}} - \Phi_{\mathbf{x}}|^2 \, d\mathbf{x} + \frac{1}{2}\int_{\Omega} \left(b_{\mathbf{x}} \cos\phi_{\mathbf{x}} - I^c_{\mathbf{x}}\right)^2 d\mathbf{x} + \frac{1}{2}\int_{\Omega} \left(b_{\mathbf{x}} \sin\phi_{\mathbf{x}} - I^s_{\mathbf{x}}\right)^2 d\mathbf{x} + \frac{\lambda}{2}\int_{\Omega} |\nabla \phi_{\mathbf{x}}|^2 \, d\mathbf{x}$$

and $I^s_{\mathbf{x}}, I^c_{\mathbf{x}}$ are the input fringe patterns obtained from the phase-shifting method, given in Equation (1); the term $b_{\mathbf{x}}$ is estimated from these fringe patterns in the following way:

$$b_{\mathbf{x}} = \sqrt{\left(I^s_{\mathbf{x}}\right)^2 + \left(I^c_{\mathbf{x}}\right)^2}.$$

The term $\Phi_{\mathbf{x}}$ is the gradient field estimated from the input fringe patterns described in Equation (3), $\Omega \subset \mathbb{R}^2$ denotes the continuous signal domain and $\lambda > 0$ is a Lagrange multiplier.

The motivation to our proposed model is twofold. First, we note that the first term in Equation (4) penalizes the differences between the known and possibly noisy gradient phase field and the recovered gradient phase field, and this term can be seen as an equivalent expression of the least-square approach to the phase unwrapping technique described in reference [5]. Also, by the action of the last term, the recovered phase field will be smoothed and the problem made well-posed. By just using these two terms, there will be many possible solutions since the gradient field of more than one phase surface will be a feasible solution. In order to avoid this problem, we inserted the second and third terms in Equation (4), to enforce the solution to be close to the input information, see Equations (1) and (3). In that sense, our model is more robust than similar models used in unwrapping processes that lack a way to constrain the solution to the expected scale and shape.

To obtain the solution of the problem expressed in Equation (4), the first-order optimality condition or Euler–Lagrange equation has to be derived. In the formal derivation, we assume that the function $\phi_{\mathbf{x}}$ is smooth enough such that gradients are well defined and the variation $\delta\phi_{\mathbf{x}}$ has compact support over Ω so that we can use the divergence theorem to get rid of the boundary term.

To simplify notation, write $\langle f \rangle = \int_\Omega f \,\mathrm{d}\mathbf{x}$ or $\langle f \rangle_\partial = \int_{\partial\Omega} f \,\mathrm{d}\mathbf{x}$ depending on whether the integral is evaluated on the domain Ω or its boundary $\partial\Omega$. Then the first variation is derived as

$$\begin{aligned}
\delta E(\phi_{\mathbf{x}}) &= \frac{1}{2}\left\langle \delta\left|\nabla\phi_{\mathbf{x}} - \Phi_{\mathbf{x}}\right|^2\right\rangle + \frac{1}{2}\left\langle \delta\left(b_{\mathbf{x}}\cos\phi_{\mathbf{x}} - I^c_{\mathbf{x}}\right)^2\right\rangle \\
&\quad + \frac{1}{2}\left\langle \delta\left(b_{\mathbf{x}}\sin\phi_{\mathbf{x}} - I^s_{\mathbf{x}}\right)^2\right\rangle + \frac{\lambda}{2}\left\langle \delta\left|\nabla\phi_{\mathbf{x}}\right|^2\right\rangle \\
&= \frac{1}{2}\left\langle 2\left(\nabla\phi_{\mathbf{x}} - \Phi_{\mathbf{x}}\right)\cdot\delta\nabla\phi_{\mathbf{x}}\right\rangle + \frac{1}{2}\left\langle 2\left(b_{\mathbf{x}}\cos\phi_{\mathbf{x}} - I^c_{\mathbf{x}}\right)\cdot\delta\left(b_{\mathbf{x}}\cos\phi_{\mathbf{x}}\right)\right\rangle \\
&\quad + \frac{1}{2}\left\langle 2\left(b_{\mathbf{x}}\sin\phi_{\mathbf{x}} - I^s_{\mathbf{x}}\right)\cdot\delta\left(b_{\mathbf{x}}\sin\phi_{\mathbf{x}}\right)\right\rangle + \frac{\lambda}{2}\left\langle 2\nabla\phi_{\mathbf{x}}\cdot\delta\nabla\phi_{\mathbf{x}}\right\rangle \\
&= \left\langle \delta\phi_{\mathbf{x}}\left(\nabla\phi_{\mathbf{x}} - \Phi_{\mathbf{x}}\right)\cdot\mathbf{n}\right\rangle_\partial - \left\langle \nabla\cdot\left(\nabla\phi_{\mathbf{x}} - \Phi_{\mathbf{x}}\right)\delta\phi_{\mathbf{x}}\right\rangle \\
&\quad + \left\langle \left(b_{\mathbf{x}}\cos\phi_{\mathbf{x}} - I^c_{\mathbf{x}}\right)\cdot\left(-b_{\mathbf{x}}\sin\phi_{\mathbf{x}}\right)\delta\phi_{\mathbf{x}}\right\rangle \\
&\quad + \left\langle \left(b_{\mathbf{x}}\sin\phi_{\mathbf{x}} - I^s_{\mathbf{x}}\right)\cdot\left(b_{\mathbf{x}}\cos\phi_{\mathbf{x}}\right)\delta\phi_{\mathbf{x}}\right\rangle \\
&\quad + \lambda\left\langle \delta\phi_{\mathbf{x}}\nabla\phi_{\mathbf{x}}\cdot\mathbf{n}\right\rangle_\partial - \lambda\left\langle \left(\nabla\cdot\nabla\phi_{\mathbf{x}}\right)\delta\phi_{\mathbf{x}}\right\rangle,
\end{aligned} \tag{5}$$

where in the last line we have used the divergence theorem and $\mathbf{n}$ denotes the unit outer normal vector to the boundary. Finally, the variational derivative of $E(\phi_{\mathbf{x}})$ is given by

$$\begin{aligned}
\frac{\partial E(\phi_{\mathbf{x}})}{\partial\phi_{\mathbf{x}}} &= -\nabla\cdot\left(\nabla\phi_{\mathbf{x}} - \Phi_{\mathbf{x}}\right) + \left(b_{\mathbf{x}}\cos\phi_{\mathbf{x}} - I^c_{\mathbf{x}}\right)\cdot\left(-b_{\mathbf{x}}\sin\phi_{\mathbf{x}}\right) \\
&\quad + \left(b_{\mathbf{x}}\sin\phi_{\mathbf{x}} - I^s_{\mathbf{x}}\right)\cdot\left(b_{\mathbf{x}}\cos\phi_{\mathbf{x}}\right) - \lambda\nabla\cdot\nabla\phi_{\mathbf{x}} \\
&= -\left(1+\lambda\right)\nabla\cdot\nabla\phi_{\mathbf{x}} + \nabla\cdot\Phi_{\mathbf{x}} + I^c_{\mathbf{x}}\cdot\left(b_{\mathbf{x}}\sin\phi_{\mathbf{x}}\right) - I^s_{\mathbf{x}}\cdot\left(b_{\mathbf{x}}\cos\phi_{\mathbf{x}}\right) = 0
\end{aligned} \tag{6}$$

with boundary conditions

$$\begin{aligned}
\left(\nabla\phi_{\mathbf{x}} - \Phi_{\mathbf{x}}\right)\cdot\mathbf{n} &= 0, \\
\nabla\phi_{\mathbf{x}}\cdot\mathbf{n} &= 0.
\end{aligned} \tag{7}$$

2.2. Numerical solution

Let $\phi_{i,j} = \phi(x_i, y_j)$ to denote the value of a grid function ϕ at point (x_i, y_j) defined on $\Omega = [a, b] \times [c, d]$ where the sampling points of the grid are

$$x_i = a + (i - 1)h_x$$
$$y_j = c + (j - 1)h_y$$

with $1 \leq i \leq m,\ 1 \leq j \leq n$, and $h_x = (b - a)/(m - 1), h_y = (d - c)/(n - 1)$.

To approximate the derivatives, we use central finite differences between ghost half-points as follows:

$$\delta_x \phi_{i,j} = \frac{\phi_{i+1/2,j} - \phi_{i-1/2,j}}{h_x} \quad \text{and} \quad \delta_y \phi_{i,j} = \frac{\phi_{i,j+1/2} - \phi_{i,j-1/2}}{h_y}.$$

The divergence term in Equation (6) is approximated as

$$\nabla \cdot V_{i,j} = \delta_x V^1_{i,j} + \delta_y V^2_{i,j},$$

where

$$V_{i,j} = (V^1_{i,j}, V^2_{i,j}) = \nabla \phi_{i,j} - \Phi_{i,j},$$
$$\nabla \phi_{i,j} = (\delta_x \phi_{i,j}, \delta_y \phi_{i,j}).$$

The rest of the terms in the equation are approximated by straight forward evaluation at point (x_i, y_j).

To implement the boundary condition on $\partial\Omega$, we assume without loss of generality that $\mathbf{n} = (\pm 1, 0)$ and $\mathbf{n} = (0, \pm 1)$ in the x and y direction, respectively. With this consideration, the first boundary condition is expressed as

$$\begin{aligned} \delta_x \phi_{m,j} - \Phi^1_{m,j} &= 0 \quad \text{for } \mathbf{n} = (1, 0), \\ -\left(\delta_x \phi_{1,j} - \Phi^1_{1,j}\right) &= 0 \quad \text{for } \mathbf{n} = (-1, 0), \\ \delta_y \phi_{i,n} - \Phi^2_{i,n} &= 0 \quad \text{for } \mathbf{n} = (0, 1), \\ -\left(\delta_y \phi_{i,1} - \Phi^2_{i,1}\right) &= 0 \quad \text{for } \mathbf{n} = (0, -1). \end{aligned} \tag{8}$$

Examples of numerical implementations of similar functionals can be found on references [4,21].

3. Numerical experiments

To illustrate the performance of the proposed method, we carried out some numerical experiments using a Intel Core i7 @ 2.40 GHz laptop with Debian GNU/Linux 8 (jessie) 64-bit and 16 GB of memory. For both experiments, we solve Equation (6) using a fast variant of Nesterov's method, which is an improvement of the gradient descent method [8,16]. In our experiments, we found that the Nesterov's method is approximately 58 times faster than the gradient descent method, as far as iterations are concerned. This method is given by

$$\begin{aligned} \beta^{k+1}_{\mathbf{x}} &= \phi^k_{\mathbf{x}} - \tau \frac{\partial E(\phi_{\mathbf{x}})}{\partial \phi_{\mathbf{x}}}, \\ t^{k+1} &= \frac{1 + \sqrt{1 + 4\left(t^k\right)^2}}{2}, \\ \phi^{k+1}_{\mathbf{x}} &= \beta^{k+1}_{\mathbf{x}} + \frac{t^k - 1}{t^{k+1}}\left(\beta^{k+1}_{\mathbf{x}} - \beta^k_{\mathbf{x}}\right) + \frac{t^k}{t^{k+1}}\left(\beta^{k+1}_{\mathbf{x}} - \phi^k_{\mathbf{x}}\right), \end{aligned} \tag{9}$$

where $\beta_{\mathbf{x}}^0 = \phi_{\mathbf{x}}^0$, $t^0 = 1$, $k = 0, 1, 2, \ldots$, and τ is the step size of the gradient descent. We chose the step size τ using the algorithm proposed in reference [24], which estimates the Lipschitz constant of the functional.

We use as stopping criteria for our optimization algorithm the same terms used in reference [29] with $\delta_1 = \delta_2 = \delta_3 = 10^{-7}$ and $k_{\max} = 15,000$. For simplicity, we selected the regularization parameter λ manually; however, well-known methods can be used to obtain the best parameter for this task, such as those described in section 5.6 of reference [1]. In addition, we use a normalized error Q to compare the phase map estimation; this error is defined as [18]

$$Q(\mu, \nu) = \frac{\|\mu - \nu\|_2}{\|\mu\|_2 + \|\nu\|_2}, \tag{10}$$

where μ and ν are the signals to be compared. The normalized error values vary between 0 (for perfect agreement) and 1 (for perfect disagreement).

3.1. Phase estimation using synthetic fringe patterns

The first set of experiments was the estimation of a synthetic phase map defined as [27]

$$\begin{aligned}\phi_{\mathbf{x}}^a = {} & 1.3 - 1.9x - 1.3\left(1 - 6y^2 - 6x^2 + 6y^4 + 12x^2y^2 + 6x^4\right) \\ & + 3.415\left(5xy^4 - 10x^3y^2 + x^5\right) \\ & + 0.43\left(3x - 12xy^2 - 12x^3 + 10xy^4 + 20x^3y^2 + 10x^5\right) \\ & + 2.6\left(-4y^3 + 12x^2y + 5y^5 - 10x^2y^3 - 15x^4\right),\end{aligned} \tag{11}$$

evaluated in a square domain $\Omega = \{(x, y) \mid -1 \leq x, y \leq 1\}$. Figure 1 shows the phase obtained from Equation (11). Figure 2 shows the fringe patterns $I_{\mathbf{x}}^c$ and $I_{\mathbf{x}}^s$ (Equation 1) used in the estimation, with resolution of 640 × 480 pixels. A first experiment was the phase estimation using the fringe patterns shown in Figure 2, where $\lambda = 1$ and the value for $\phi_{\mathbf{x}}^0$ was randomly generated. The estimated phase map is shown in Figure 3. The normalized error was $Q = 0.0014$ and the time employed to obtain the solution was 106 s using 2342 iterations of the Nesterov's method (Equation 9). Figure 4 shows the error obtained in this estimation.

A second estimation was made using fringe patterns with SNR = 12.5 db [6], shown in Figure 5. For this estimation, we use $\lambda = 1.0$ and the initial value was randomly generated. The estimated phase

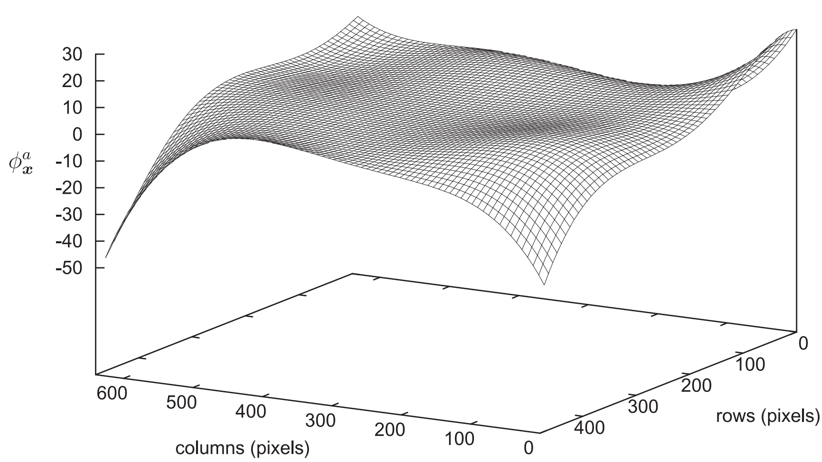

Figure 1. Synthetic phase map given in Equation (11).

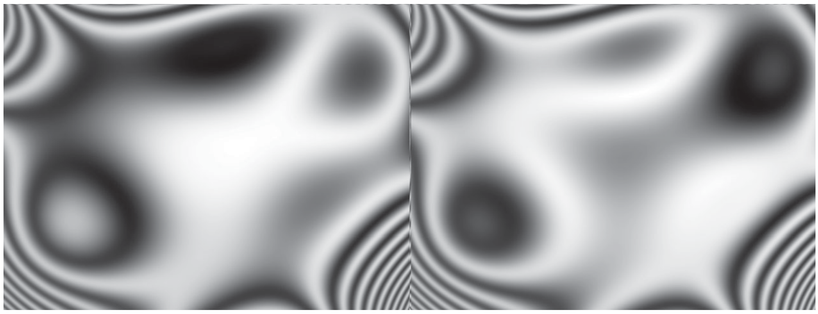

Figure 2. Fringe patterns generated with the phase map given in Equation (11): (a) $I^c_{\mathbf{x}}$ and (b) $I^s_{\mathbf{x}}$.

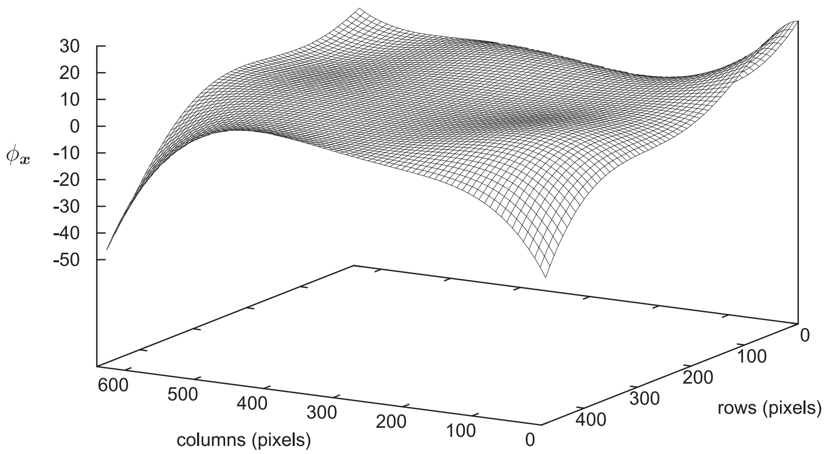

Figure 3. Estimated phase map using fringe patterns shown in Figure 2.

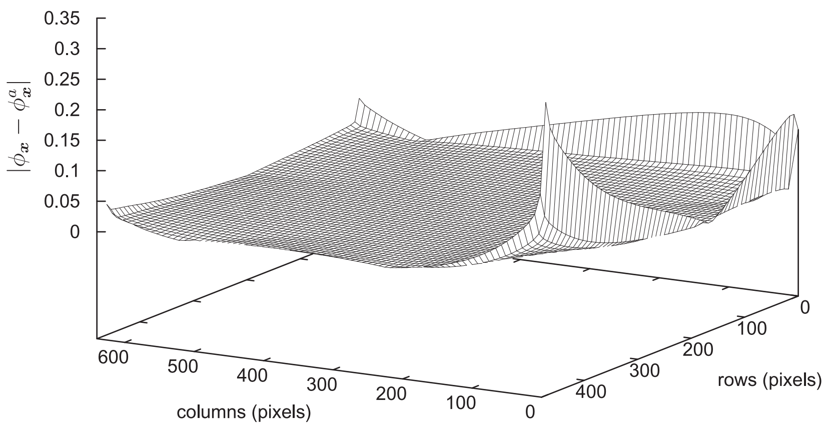

Figure 4. Absolute difference between the estimated phase map using fringe patterns shown in Figure 2 and the synthetic phase map given in Equation (11).

map is shown in Figure 6. The normalized error was $Q = 0.016$ and the time employed to obtain the solution was 123 s using 2819 iterations of the Nesterov's method. Figure 7 shows the error obtained in this estimation. Table 1 presents a summary of the estimation performance of our proposed functional using the fringes patterns generated by Equation (11) with different SNR.

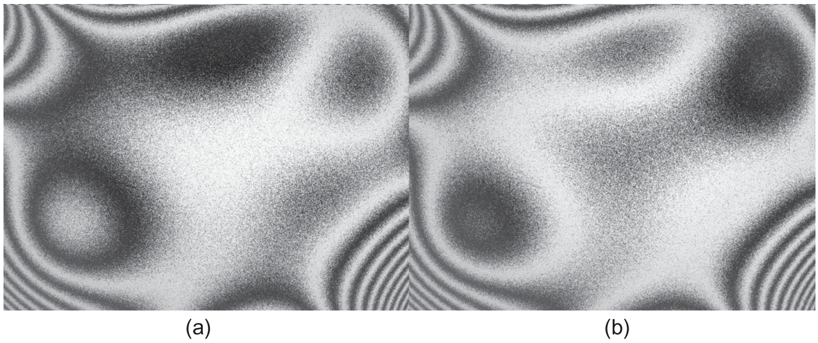

Figure 5. Noisy fringe patterns generated with the phase map given in Equation (11): (a) $I^c_{\mathbf{x}}$ and (b) $I^s_{\mathbf{x}}$.

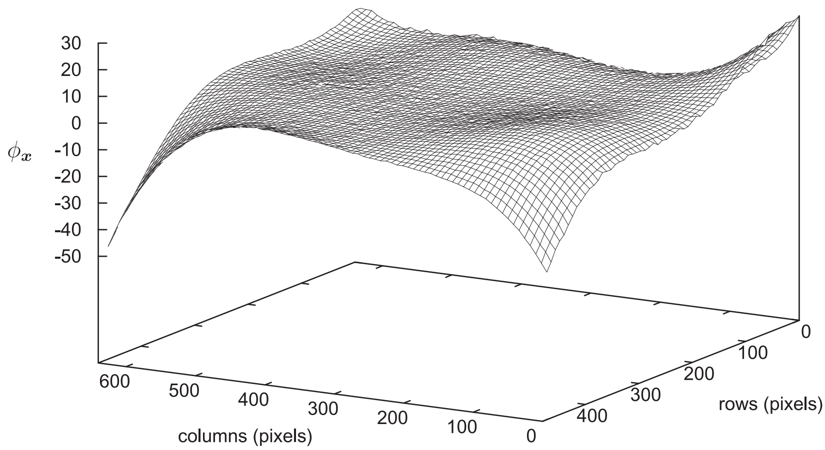

Figure 6. Estimated phase map using fringe patterns shown in Figure 5.

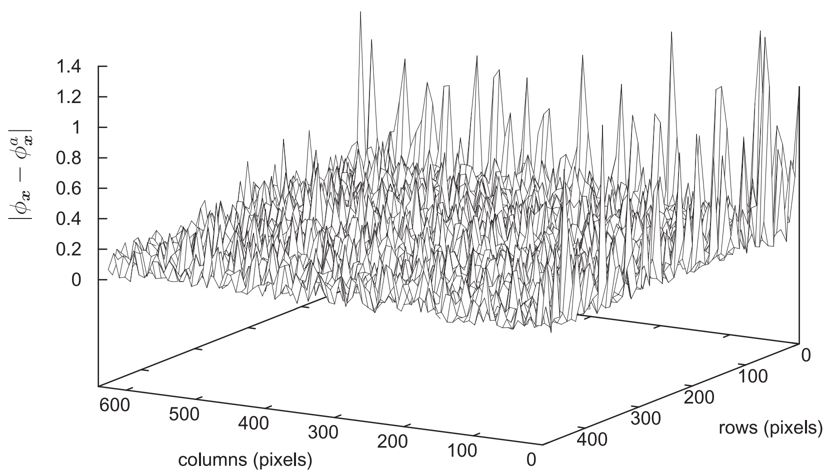

Figure 7. Absolute difference between the estimated phase map using fringe patterns shown in Figure 5 and the synthetic phase map given in Equation (11).

Table 1. Estimation performance of Equation (4) using fringe patterns generated with Equation (11).

SNR (db)	Iterations	Normalized error (Q)
inf	2342	0.00142
39.97	2428	0.00335
27.98	2483	0.00980
21.08	2501	0.00867

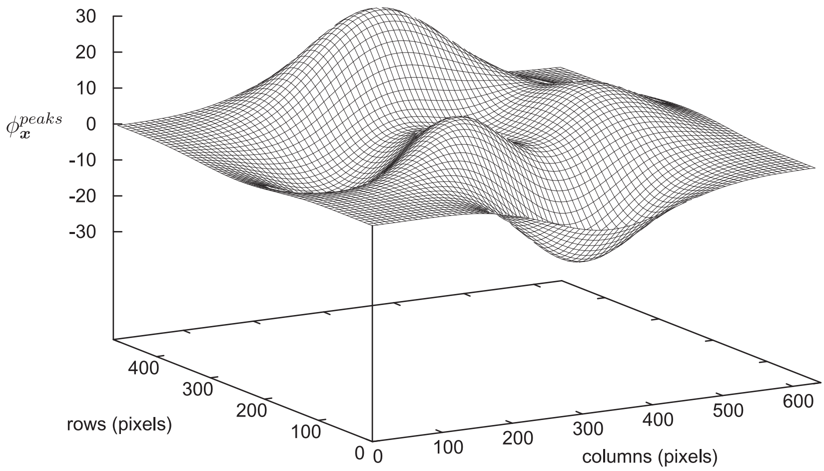

Figure 8. Synthetic phase map given by `peaks` function.

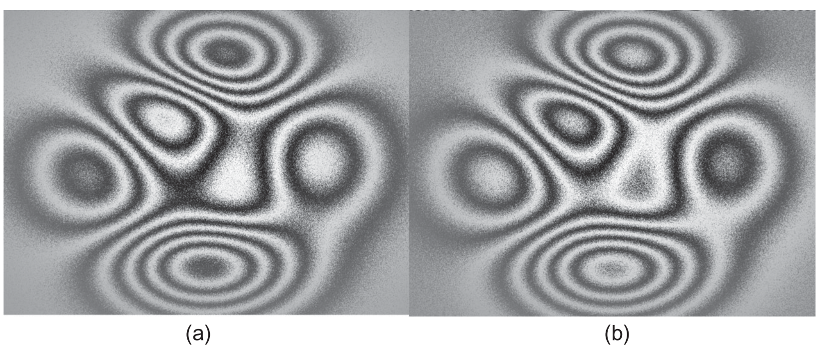

Figure 9. Noisy fringe patterns generated with the phase map given in Figure 8: (a) $I^c_{\mathbf{x}}$ and (b) $I^s_{\mathbf{x}}$.

A second experiment was the estimation of a synthetic phase map defined by the MATLAB `peaks` function [2], evaluated in a square domain $\Omega = \{(x, y) \mid -2.3 \leq x, y \leq 2.3\}$. Figure 8 shows the wrapped phase generated by the `peaks` function, and Figure 9 shows the fringe patterns $I^c_{\mathbf{x}}$ and $I^s_{\mathbf{x}}$ (Equation 1) used in the estimation, with resolution of 640×480 pixels with SNR $= 12.7$ db. The resultant estimated phase map is shown in Figure 10 where the normalized error was $Q = 0.014$ and the time employed to obtain the solution was 342 s using 7552 iterations of the Nesterov's method. Figure 11 shows the error obtained in this estimation. Table 2 presents a summary of the estimation performance of our proposed functional using the fringe patterns generated by the MATLAB `peaks` function with different SNR.

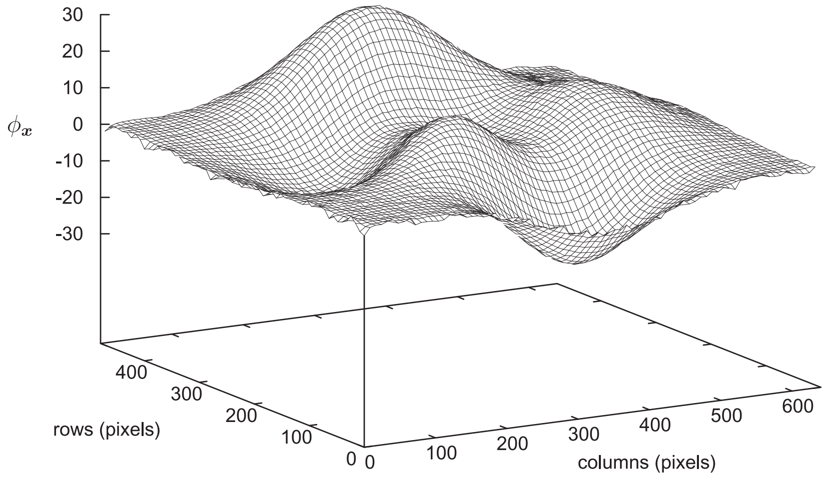

Figure 10. Estimated phase map using fringe patterns shown in Figure 9.

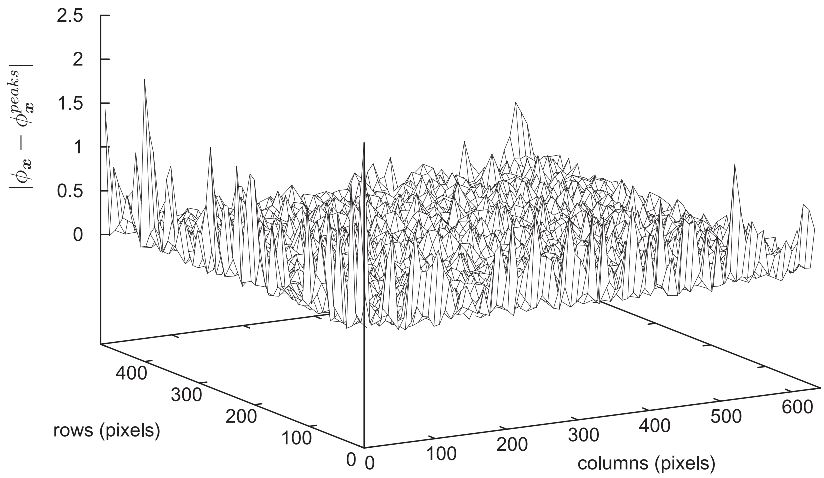

Figure 11. Absolute difference between the estimated phase map using fringe patterns shown in Figure 9 and the synthetic phase map given by `peaks` function.

Table 2. Estimation performance of Equation (4) using fringe patterns generated with `peaks` function.

SNR (db)	Iterations	Normalized error (Q)
inf	5555	0.00072
40.26	5876	0.00366
28.22	6350	0.00603
21.22	6782	0.00823
14.44	7349	0.01076
12.72	7552	0.01427

3.2. Phase estimation using experimental fringe patterns

In this experiment, we show the performance of the proposed method on the processing of experimental information with noise. This experiment consists of the phase estimation of a sequence of five fringe patterns obtained from a holographic interferometric experiment [9]. Figure 12 shows the

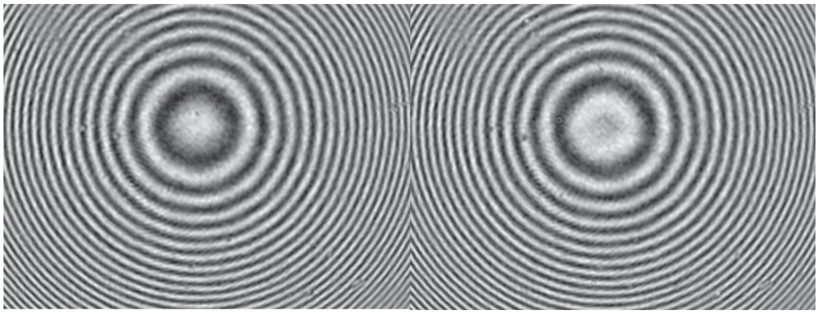
(a) (b)

Figure 12. Experimental fringe patterns: (a) $I_{\mathbf{x}}^{c}$ and (b) $I_{\mathbf{x}}^{s}$.

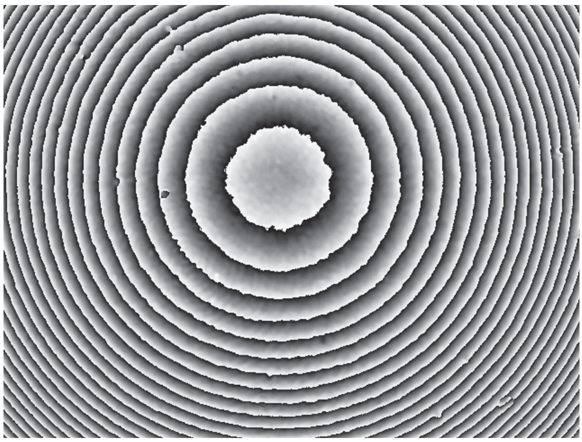

Figure 13. Wrapped phase map generated by the fringe patterns shown in Figure 12.

fringe patterns $I_{\mathbf{x}}^{c}$ and $I_{\mathbf{x}}^{s}$ (Equation 1) obtained from the phase-shifting method, with the resolution of 640 × 480 pixels. The wrapped phase map obtained from these fringe patterns can be observed in Figure 13.

Due to the noisy phase term, the strong variations in the modulation or the presence of phase-shift miscalibration [25], the iterative process will be slow or even trapped on a local minimum. To improve the iterative process, we propose to use as initial value the phase term obtained from the method reported in reference [17]. Figure 14 shows the estimated phase using $\lambda = 1.5$; the normalized error was $Q = 0.012$ and the time employed to obtain the solution was 87 s, including the time employed to estimate the initial value, using 1590 iterations of the Nesterov's method.

To compare the performance of our proposal, we unwrap the phase map shown in Figure 13 with two unwrapping methods: (a) the discrete version of Poisson equation (Equation 5.31 of reference [5]) and (b) the method described in reference [15]. For both cases, we used the Nesterov's method as optimization technique. Figure 15 shows the estimated phase using reference [5], where the time employed to obtain the solution was 40 s, including the time employed to estimate the initial value, using 5205 iterations of the Nesterov's method and the normalized error was $Q = 0.015$. Figure 16 shows the estimated phase using reference [15] with $\lambda = 1.2$, where the time employed to obtain the solution was 245 s, including the time employed to estimate the initial value, using 15,000 iterations of the Nesterov's method and the normalized error was $Q = 0.241$.

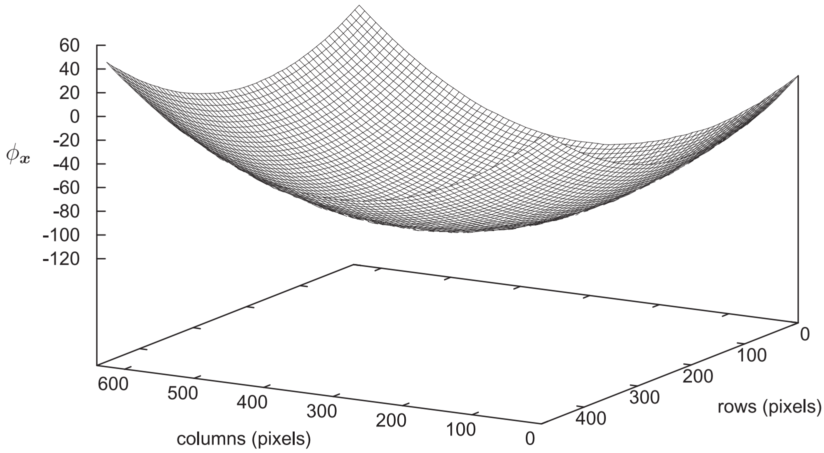

Figure 14. Estimated phase map using Equation (4).

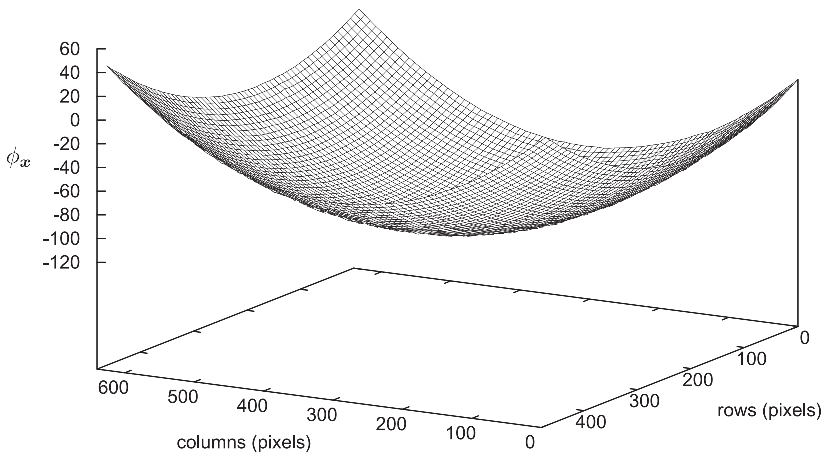

Figure 15. Estimated phase map using Equation (5.31) of reference [5].

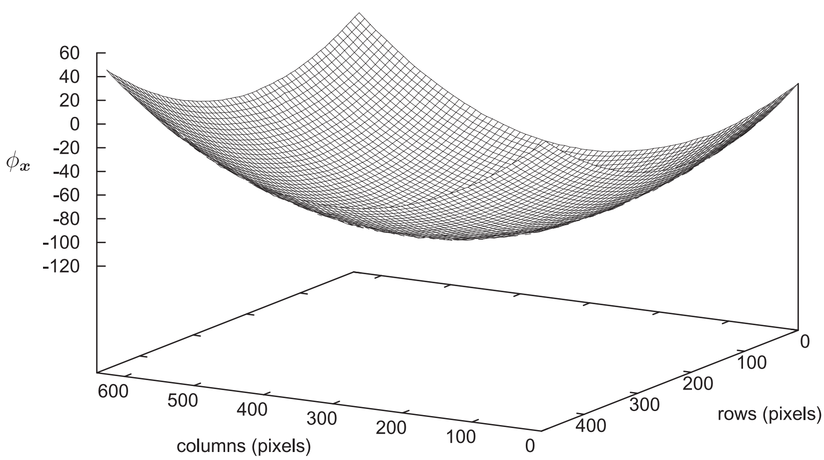

Figure 16. Estimated phase map using reference [15].

4. Discussion of results and conclusion

As can be observed from the above experiments, the proposed method successfully estimates the unwrapped phase map from the information of the phase-shifting method methods; that is, the fringe patterns $I^c_{\mathbf{x}}$ and $I^s_{\mathbf{x}}$, without the use of the wrapped phase map. This method converges to an accurate solution given an arbitrary initial point, even for noisy fringe patterns. Due to the smoothing term included in the functional, it is possible to obtain a filtered phase map with the preservation of the dynamic range of the fringe patterns.

The numerical solution of Equation (4) results on a very simple algorithm which estimate a filtered phase map in a short time, despite the optimization algorithm with poor convergence rate used in experiments. In comparison with the methods described in reference [5] (Equation 5.31) and reference [15], the proposed method shows a good performance on the estimation and the computational load employed to compute the phase map. To improve the convergence rate, the proposed method can be easily implemented with a better computationally efficient techniques, including parallel approaches. This will be one aim of our future research.

Disclosure statement

No potential conflict of interest was reported by the authors.

ORCID

Ricardo Legarda-Saenz http://orcid.org/0000-0003-4875-324X
Alejandro Téllez Quiñones http://orcid.org/0000-0001-6712-0582
Carlos Brito-Loeza http://orcid.org/0000-0003-2970-2113
Arturo Espinosa-Romero http://orcid.org/0000-0002-5153-2950

References

[1] M. Bertero and P. Boccacci, *Introduction to Inverse Problems in Imaging*, Institute of Physics Publishing, Bristol, 1998.
[2] T.A. Davis, *MATLAB Primer*, 8th ed., CRC Press, Boca Raton, Fl, 2014.
[3] K.J. Gasvik, *Optical Metrology*, 3rd ed., John Wiley & Sons, Chichester, 2002.
[4] P. Getreuer, *Rudin–Osher–Fatemi total variation denoising using split Bregman*, Image Process 2012 (2012), pp. 1–20. Available at http://dx.doi.org/10.5201/ipol.2012.g-tvd.
[5] D.C. Ghiglia and M.D. Pritt, *Two-Dimensional Phase Unwrapping: Theory, Algorithms, and Software*, Wiley-Interscience, New York, 1998.
[6] R.C. Gonzalez and R.E. Woods, *Digital Image Processing*, 3rd ed., Pearson Prentice Hall, Upper Saddle River, NJ, 2008.
[7] H.Y.H. Huang, L. Tian, Z. Zhang, Y. Liu, Z. Chen, and G. Barbastathis, *Path-independent phase unwrapping using phase gradient and total-variation (TV) denoising*, Opt. Express. 20 (2012), pp. 14075–14089. Available at http://dx.doi.org/10.1364/OE.20.014075.
[8] D. Kim and J.A. Fessler, *Optimized first-order methods for smooth convex minimization*, Math. Program. 159 (2016), pp. 81–107. Available at http://dx.doi.org/10.1007/s10107-015-0949-3.
[9] T. Kreis, *Holographic Interferometry: Principles and Methods*, Wiley-VCH, Berlin, 1996.
[10] C. Lacombe, P. Kornprobst, G. Aubert, and L. Blanc-Feraud, *A variational approach to one dimensional phase unwrapping*, in *16th International Conference on Pattern Recognition, 2002*, Vol. 2. 2002, pp. 810–813. Available at http://dx.doi.org/10.1109/ICPR.2002.1048426.
[11] R. Legarda-Saenz, W. Osten, and W.P. Juptner, *Improvement of the regularized phase tracking technique for the processing of nonnormalized fringe patterns*, Appl. Opt. 41 (2002), pp. 5519–5526. Available at http://dx.doi.org/10.1364/AO.41.005519.
[12] R. Legarda-Saenz, C. Brito-Loeza, and A. Espinosa-Romero, *Total variation regularization cost function for demodulating phase discontinuities*, Appl. Opt. 53 (2014), p. 2297. Available at http://dx.doi.org/10.1364/AO.53.002297.
[13] B. Li, C. Tang, G. Gao, M. Chen, S. Tang, and Z. Lei, *General filtering method for electronic speckle pattern interferometry fringe images with various densities based on variational image decomposition*, Appl. Opt. 56 (2017), p. 4843. Available at https://doi.org/10.1364/AO.56.004843.
[14] D. Malacara, M. Servín, and Z. Malacara, *Interferogram Analysis for Optical Testing*, 2nd ed., CRC Press, Boca Raton, Fl, 2005. Available at http://dx.doi.org/10.1201/9781420027273.fmatt.

[15] J.L. Marroquin and M. Rivera, *Quadratic regularization functionals for phase unwrapping*, J. Opt. Soc. Amer. A 12 (1995), pp. 2393–2400. Available at http://dx.doi.org/10.1364/JOSAA.12.002393.

[16] B. O'Donoghue and E. Candes, *Adaptive restart for accelerated gradient schemes*, Found. Comput. Math. 15 (2015), pp. 715–732. Available at http://dx.doi.org/10.1007/s10208-013-9150-3.

[17] G. Paez and M. Strojnik, *Phase-shifted interferometry without phase unwrapping: Reconstruction of a decentered wave front*, J. Opt. Soc. Amer. A 16 (1999), p. 475. Available at https://doi.org/10.1364/JOSAA.16.000475.

[18] M. Perlin and M.D. Bustamante, *A robust quantitative comparison criterion of two signals based on the Sobolev norm of their difference*, J. Eng. Math. 101 (2016), pp. 115–124. Available at http://dx.doi.org/10.1007/s10665-016-9849-7.

[19] G. Rajshekhar and P. Rastogi, *Fringe analysis: Premise and perspectives*, Opt. Lasers Eng. 50 (2012), pp. iii–x. Available at http://dx.doi.org/10.1016/j.optlaseng.2012.04.006.

[20] D.W. Robinson and G.T. Reid, *Interferogram Analysis: Digital Fringe Pattern Measurement Techniques*, Institute of Physics Publishing, Bristol, 1993.

[21] L.I. Rudin, S. Osher, and E. Fatemi, *Nonlinear total variation based noise removal algorithms*, Phys. D 60 (1992), pp. 259–268. Available at http://dx.doi.org/10.1016/0167-2789(92)90242-F.

[22] M. Servin, J.L. Marroquin, and F.J. Cuevas, *Demodulation of a single interferogram by use of a two-dimensional regularized phase-tracking technique*, Appl. Opt. 36 (1997), pp. 4540–8. Available at http://dx.doi.org/10.1364/AO.36.004540.

[23] M. Servin, J.A. Quiroga, and M. Padilla, *Fringe Pattern Analysis for Optical Metrology: Theory, Algorithms, and Applications*, Wiley, Weinheim, 2014.

[24] Z.J. Shi and J. Shen, *Step-size estimation for unconstrained optimization methods*, Comput. Appl. Math. 24 (2005), pp. 399–416. Available at https://doi.org/10.1590/S0101-82052005000300005.

[25] Y. Surrel, *Design of algorithms for phase measurements by the use of phase stepping*, Appl. Opt. 35 (1996), pp. 51–60. Available at http://dx.doi.org/10.1364/AO.35.000051.

[26] A. Tellez-Quinones and D. Malacara-Doblado, *Inhomogeneous phase shifting: An algorithm for nonconstant phase displacements*, Appl. Opt. 49 (2010), pp. 6224–6231. Available at http://dx.doi.org/10.1364/AO.49.006224.

[27] A. Tellez-Quinones and D. Malacara-Doblado, *Phase recovering without phase unwrapping in phase-shifting interferometry by cubic and average interpolation*, Appl. Opt. 51 (2012), pp. 1257–1265. Available at http://dx.doi.org/10.1364/AO.51.001257.

[28] A. Tellez-Quinones, D. Malacara-Doblado, and J. Garcia-Marquez, *Polynomial fitting model for phase reconstruction: Interferograms with high fringe density*, in *Proceeding of the SPIE*, J. Schmit, K. Creath, C.E. Towers, and J. Burke, eds., Vol. 8493, Sep. 2012, p. 849319. Available at http://dx.doi.org/10.1117/12.956500.

[29] C.R. Vogel and M.E. Oman, *Iterative methods for total variation denoising*, SIAM J. Sci. Comput. 17 (1996), pp. 227–238. Available at http://dx.doi.org/10.1137/0917016.

[30] K. Yatabe and Y. Oikawa, *Convex optimization-based windowed Fourier filtering with multiple windows for wrapped-phase denoising*, Appl. Opt. 55 (2016), p. 4632. Available at http://dx.doi.org/10.1364/AO.55.004632.

[31] K. Yatabe, K. Ishikawa, and Y. Oikawa, *Improving principal component analysis based phase extraction method for phase-shifting interferometry by integrating spatial information*, Opt. Express. 24 (2016), p. 22881. Available at http://dx.doi.org/10.1364/OE.24.022881.

[32] K. Yatabe, K. Ishikawa, and Y. Oikawa, *Hyper ellipse fitting in subspace method for phase-shifting interferometry: Practical implementation with automatic pixel selection*, Opt. Express. 25 (2017), p. 29401. Available at https://doi.org/10.1364/OE.25.029401.

[33] K. Yatabe, K. Ishikawa, and Y. Oikawa, *Simple, flexible, and accurate phase retrieval method for generalized phase-shifting interferometry*, J. Opt. Soc. Amer. A 34 (2017), p. 87. Available at https://doi.org/10.1364/JOSAA.34.000087.

[34] F. Zhang, W. Liu, C. Tang, J. Wang, and L. Ren, *Variational denoising method for electronic speckle pattern interferometry*, Chin. Opt. Lett. 6 (2008), pp. 38–40. Available at http://dx.doi.org/10.3788/COL20080601.0038.

[35] X. Zhu, Z. Chen, and C. Tang, *Variational image decomposition for automatic background and noise removal of fringe patterns*, Opt. Lett. 38 (2013), pp. 275–277. Available at http://dx.doi.org/10.1364/OL.38.000275.